

Nitrogen composition dependence of electron effective mass in GaAs_{1-x}N_x

T. Dannecker,^{1,2,3} Y. Jin,^{2,3} H. Cheng,³ C. F. Gorman,² J. Buckeridge,¹ C. Uher,³ S. Fahy,^{1,3} C. Kurdak,³ and R. S. Goldman^{2,3,*}

¹Tyndall National Institute, University College Cork, Cork, Ireland

²Department of Materials Science and Engineering, University of Michigan, Ann Arbor, Michigan 48109-2136, USA

³Department of Physics, University of Michigan, Ann Arbor, Michigan 48109-1040, USA

(Received 3 February 2010; revised manuscript received 14 July 2010; published 3 September 2010; corrected 20 October 2010)

We have investigated the N composition, x , and temperature, T , dependence of the electron effective mass, m^* , of GaAs_{1-x}N_x films with sufficiently low carrier concentration that carriers are expected to be confined to near the bottom of the conduction-band edge (CBE). Using Seebeck and Hall measurements, in conjunction with assumptions of parabolic bands and Fermi-Dirac statistics, we find a nonmonotonic dependence of m^* on x and an increasing T dependence of m^* with x . These trends are not predicted by the two-state band anticrossing model but instead are consistent with the predictions of the linear combination of resonant nitrogen states model, which takes into account several N-related states and their interaction with the GaAs CBE.

DOI: 10.1103/PhysRevB.82.125203

PACS number(s): 72.20.Pa, 72.20.My, 71.18.+y, 81.05.Ea

I. INTRODUCTION

Dilute nitride alloys such as GaAsN and InGaAsN are promising for a wide range of applications including laser diodes, high-efficiency solar cells, and high performance bipolar transistors. Earlier studies have shown that the electron mobility of (In)GaAs_{1-x}N_x decreases significantly with N composition, x ,¹⁻⁶ presumed to be partly due to the influence of N incorporation on the effective mass, m^* .^{3,4,7,8} There have been conflicting experimental^{3,7-9} and theoretical^{8,10,11} reports on the x and temperature, T , dependences of m^* . For $x < 0.005$, m^* was reported to either decrease⁴ or rapidly increase^{3,7,9} with increasing x . For $x > 0.005$, m^* is predicted to either increase monotonically, according to the simple band anticrossing (BAC) model,¹¹ or to vary nonmonotonically with a minimum around $x=0.01$ and a maximum around $x=0.02$, according to the linear combination of resonant nitrogen states (LCINS) model.¹⁰ However, experimentally, a x -dependent saturation in m^* was reported.⁷ In terms of the T dependence, one group has reported measurements showing that m^* decreases monotonically with increasing T .⁸ Here, we have determined the x dependence of m^* , using a combination of T -dependent Seebeck and Hall measurements, interpreted in the framework of parabolic conduction bands and Fermi-Dirac statistics. We find a nonmonotonic behavior of m^* with x . Our results are in contrast to the prediction of a simple BAC model¹¹ of a monotonic decrease in m^* with increasing x , but they are very similar to the predicted minimum at $x=0.01$ of the LCINS model¹⁰ and to the experimental values for $x=0.016$ of Ibáñez *et al.*³ In addition, our data suggest a more significant T dependence with m^* decreasing by $\sim 30\%$ from 150 to 300K.

II. EXPERIMENTS

For these studies, GaAs_{1-x}N_x alloy films were grown on (001) GaAs substrates by molecular-beam epitaxy, using Ga, As, GaTe, and a N₂ radio-frequency plasma source with ultrahigh-purity N₂ gas, as described elsewhere.^{5,12} For all samples, a 500-nm-thick buffer layer was grown at 580 °C

on GaAs (001) substrates using a growth and annealing sequence described elsewhere.¹³ Next, an electronically active layer of GaAs(N) was grown at 400 °C with targeted Te doping concentrations of $5-13 \times 10^{17}$ cm⁻³. The buffer and active layers were grown with As to Ga incorporation rate ratios of 1.5.¹⁴ In all cases, the surface reconstruction was monitored *in situ* with reflection high-energy electron diffraction.

Following growth, x in the GaAs_{1-x}N_x films was determined using x-ray rocking curves, interpreted with an interstitial model, as discussed elsewhere.¹⁵ For Hall and magnetotransport measurements, Hall bars (1050×150 μm²) were prepared using standard lithography and lift-off processes. For thermoelectric measurements, 5 mm \times 15 mm rectangles were cleaved and In-Sn contacts were applied, and subsequently annealed at 410 °C for 2 min in N₂ atmosphere.

To determine the carrier concentration, we measured the parallel resistivity, ρ_{xx} , and the transverse resistivity, ρ_{xy} , as a function of T (1.6 to 300 K) and magnetic field (-8 to 8 T). For measurements of the Seebeck coefficient, $S = \Delta V / \Delta T$, a current-driven heater and a copper block were attached to each end of the cleaved rectangles. The thermally induced T gradients were measured with thermocouples attached to the In-Sn contacts.

III. RESULTS AND DISCUSSION

Figure 1 shows a plot of S as function of T , from 2 to 300 K, for GaAs and GaAsN layers. At the lowest T , S decreases monotonically to a minimum (maximum absolute value) at 12 K, followed by a corresponding monotonic increase up to ~ 100 K. The significant enhancement of $|S|$ in the low- T regime is attributed to increased electron-phonon coupling, often termed the “phonon drag” component of S .¹⁶ For GaAs_{1-x}N_x with $x=0$, the maximum $|S|$ is 1000 μV K⁻¹, and increases with x , from 1800 to 3050 μV K⁻¹ for $x=0.01$ to $x=0.017$.

For $T > 140$ K, for both GaAs and GaAsN, S decreases monotonically with T , due to electron diffusion driven by the

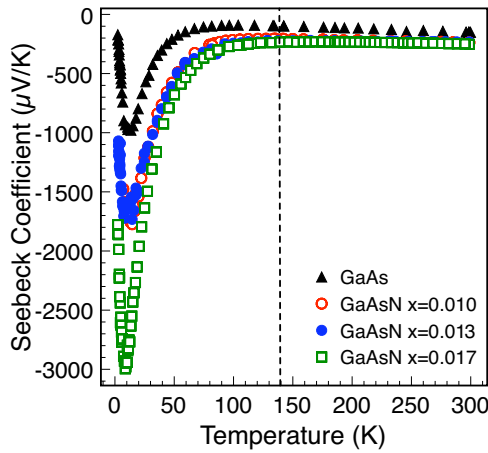


FIG. 1. (Color online) Seebeck coefficient, S , as a function of temperature, T , from 2 to 300 K. The significant enhancement in $|S|$ in the low- T regime is attributed to increased electron-phonon coupling, often termed phonon drag. For the T range from 140 to 300 K, $|S|$ decreases monotonically with T , due to electron diffusion driven by the T gradient.

T gradient. To consider the influence of x on S in this so-called “diffusion” regime, we examine S in the T range from 140 to 300 K, shown in Fig. 2(a). For GaAs, S is negative and decreases monotonically with increasing T , consistent with reported values for n -type GaAs.¹⁷ In the GaAsN alloys, S is also negative and decreases monotonically with increasing T . However, the absolute values of S are larger than those of GaAs and the T dependence is less significant. In Fig. 2(a), linear least-squares fits to $S(T)$ are shown. For each value of x in $\text{GaAs}_{1-x}\text{N}_x$, the electron diffusion regime is identified within this T range. Interestingly, the low- T bound of the electron diffusion regime increases with x , from 140 K for GaAs to nearly 200 K for $\text{GaAs}_{1-x}\text{N}_x$ with $x=0.017$. Since S consists of a phonon drag, S_{ph} , and a electron diffusion, S_{el} , component, the total is $S=S_{ph}+S_{el}$. With increasing x , the phonon drag component, S_{ph} , increases, and the S_{ph} tail extends to higher T , presumably due to a shift of the electron diffusion regime to higher T .

As shown in Fig. 2(b), the GaAs free carrier concentration, n_s , is T independent. For GaAsN alloys grown with nominally identical doping concentration, n_s is approximately an order of magnitude lower than that of GaAs, presumably due to electron trapping at native N-related defect states, e.g., N interstitials.^{12,18,19} In addition, for all the GaAsN alloys, n_s exhibits a gradual monotonic increase with temperature, suggesting the presence and thermal activation of deep-level donors related to N interstitials.¹⁸ In all cases, n_s is sufficiently low that carriers are expected to be confined to near the bottom of the conduction-band edge (CBE). Indeed, the Fermi level, derived using Eq. (2) (below), is within ± 20 meV of the CBE, varying from +20 meV ($x=0.001$) to -20 meV ($x=0.019$). Therefore, any nonparabolicity of the CBE is expected to be negligible.

To determine the values of m^* , S is defined in terms of the reduced Fermi level, $\eta=E_F/k_B T$, where E_F is the Fermi level with respect to the CBE, and the electron momentum relaxation time τ_m , as follows:

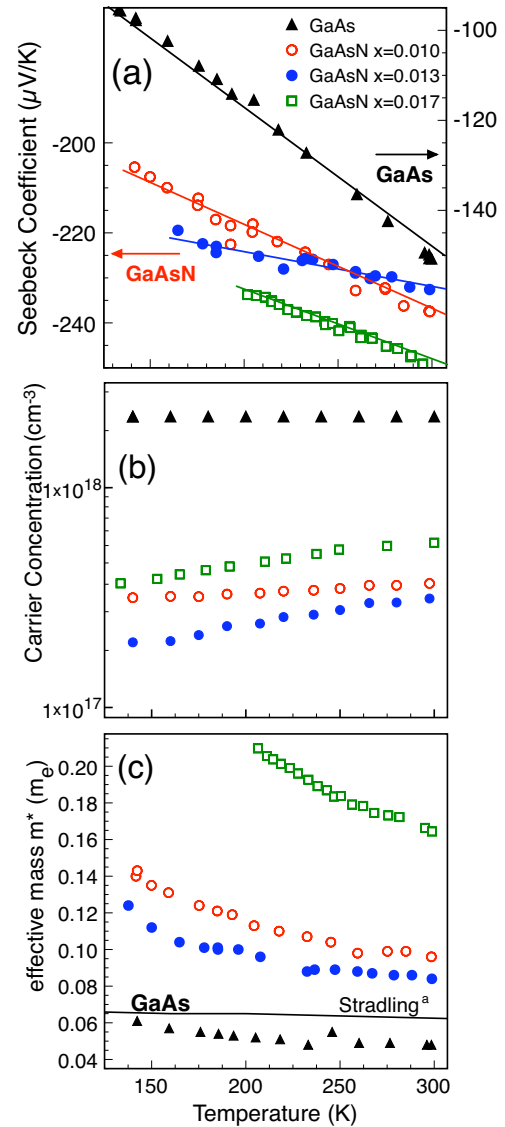


FIG. 2. (Color online) Electronic properties as a function of temperature, T , are shown from 135 to 300 K. (a) Seebeck coefficient, S , for $\text{GaAs}_{1-x}\text{N}_x$ (left axis) and GaAs (right axis). Linear least-square fits to the data are shown. The low- T bound of the electron diffusion regime increases with x , from 140 K for GaAs to nearly 200 K for $\text{GaAs}_{1-x}\text{N}_x$ with $x=0.017$. (b) Free carrier concentration, n_s , for $\text{GaAs}_{1-x}\text{N}_x$, and (c) m^* determined from S and n_s using assumptions of parabolic bands and Fermi-Dirac statistics.^aSee Ref. 33.

$$S = \frac{k_B}{e} \left(\frac{\langle \tau_m \eta \rangle}{\langle \tau_m \rangle} - \eta \right). \quad (1)$$

In general, τ_m is a function of the reduced Fermi level $\tau_m = \tau_0 \eta^r$, where $r=3/2$ for ionized impurity scattering (GaAs) (Ref. 20) and $r=-1/2$ for localized N scattering (GaAsN).⁵ We note that the introduction of N into GaAs has been reported to lead to an order of magnitude decrease in electron mobility.^{2,3,5,8,18,21} Since the majority of N is incorporated substitutionally, it is thus assumed that electrons in GaAsN are primarily scattered by localized states associated

with N atoms. Furthermore, LO phonon scattering in GaAs has been reported to be insignificant at room temperature (RT) and to decrease with decreasing temperature,^{22,23} therefore, it is not expected to be significant in GaAsN at low T . S is then simplified to

$$S = \frac{k_B}{e} \left[\frac{(r+5/2) F_{r+3/2}(\eta)}{(r+3/2) F_{r+1/2}(\eta)} - \eta \right], \quad (2)$$

where $F_j(\eta)$ is the j th Fermi integral given as

$$F_j(\eta) = \frac{1}{j!} \int_0^\infty \frac{E^j}{e^{(E-E_F)/k_B T} + 1} dE. \quad (3)$$

Using Fermi-Dirac statistics, the free carrier concentration is written as

$$n = 2 \left(\frac{m^* k_B T}{2\pi\hbar^2} \right)^{3/2} F_{1/2}(\eta) \quad (4)$$

and the effective mass becomes

$$m^* = \frac{2\pi\hbar^2}{k_B T} \left[\frac{n}{2F_{1/2}(\eta)} \right]^{2/3}. \quad (5)$$

For GaAs, using the values of S and n , shown in Figs. 2(a) and 2(b), and solving for η in Eqs. (2) and (5), we find a RT value of m^* of 0.048 ± 0.019 times the free-electron mass (m_e) and a monotonic decrease in m^* with increasing T (19% from 140 to 300 K), as shown in Fig. 2(c). Similar RT values of m^* were obtained by other groups using indirect experimental methods, including analysis of electric susceptibility and Shubnikov de Haas measurements.^{24–26} However, a larger RT m^* value, $0.067m_e$, was observed via direct experimental methods, such as cyclotron resonance, Faraday rotation, and Faraday oscillation.^{27–30} In addition, a significantly smaller gradient in the monotonic T -dependent decrease in m^* is typically observed,^{27,30–32} consistent with the calculations of the dilatational change in the energy gap in GaAs by Stradling and Wood.³³ Overall, at room temperature, our GaAs m^* is within 20% of literature values, and the estimated error in m^* , $\pm 0.019m_e$, is negligible compared to the variations in the GaAsN m^* (from $0.084m_e$ to $0.164m_e$).

For GaAsN, m^* is larger than that of GaAs, and decreases monotonically with increasing T . Similar low- T values for m^* in GaAsN were reported in Refs. 7 and 9. The significant T dependence of m^* in GaAsN is likely due to a nonparabolic perturbation in the electron dispersion relation, leading to a local increase in m^* . In PbTeTl,³⁴ a similar temperature dependence of S and m^* were reported, and attributed to an isolated Tl energy level in close proximity to the PbTe CBE. In addition, a maximum of m^* was observed at 230 K and attributed to a resonance between the Tl state and the PbTe CBE.

In both GaAs and GaAsN, it appears that the phonon drag component of S (for $T < 150$ K), shown in Fig. 1, contributes to a small artificial increase in m^* . Indeed, significant decreases in S are observed for $T < 150$ K with the most significant decreases for $T < 100$ K. The lower S value leads to an increase in E_f , and a subsequently smaller m^* [see Eqs. (2) and (5)].

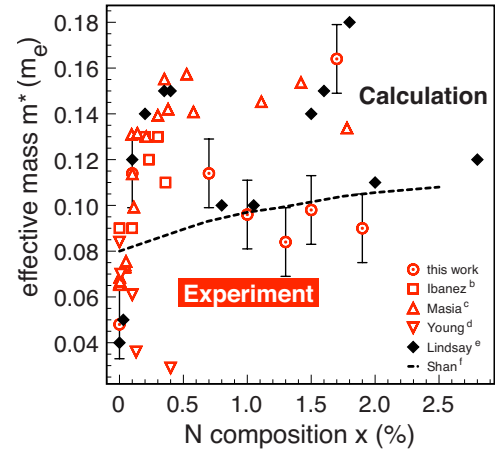


FIG. 3. (Color online) Effective mass, m^* , vs N composition, x , for as-grown bulk $\text{GaAs}_{1-x}\text{N}_x$. “This work” values are given at RT; Ibáñez *et al.* are extracted by Raman spectroscopy at 80 K; Masia *et al.* from magnetophotoluminescence at 20 K; Young *et al.* from magnetotransport at RT; Lindsay *et al.* from the LCINS model at low T ; and Shan *et al.* (dashed line) from the two-state BAC model at low T . ^bSee Ref. 3. ^cSee Ref. 7. ^dSee Ref. 4. ^eSee Ref. 10. ^fSee Ref. 11.

The influence of x on m^* is shown in Fig. 3. For $x < 0.005$, an increase in the m^* with increasing x up to $x=0.04$,^{3,7} and subsequent saturation beyond $x=0.005$ (Ref. 7) have been reported experimentally. The rapid increase up to $x=0.004$ is in good agreement with the predictions of the LCINS model.^{7,10} For $x > 0.005$, the LCINS model predicts nonmonotonic behavior of m^* with increasing x , with a minimum at $x=0.010$ and a maximum at $x=0.018$. The oscillatory dependence of m^* on x was explained by a strong hybridization of states arising from N clusters near the CBE of GaAs,¹⁰ leading to a large locally increased m^* in GaAsN.

Our RT m^* values for $\text{GaAs}_{1-x}\text{N}_x$ films are in good agreement with low-temperature values predicted by the LCINS model¹⁰ and those from other experimental reports.^{3,7} For a limited composition range ($x=0.010$ – 0.015), our RT m^* values are also in agreement with those predicted by the BAC model.¹¹ Indeed, the temperature dependence of m^* is apparently negligible. As the temperature is reduced from 300 to 0 K, the relative energies of the nitrogen-induced localized states and the CBE are shifted by approximately 36 meV.⁶ Since the x values investigated range from 0.001 to 0.019, a negligible temperature dependence of the x values at which the localized state-CBE resonance induced increase in effective mass is expected.

For the lowest x values, $x=0.001$ and $x=0.006$ ($m^*=0.114m_e$) is consistent with the maximum at $x=0.005$ ($m^*=0.15m_e$), predicted by the LCINS model. In addition, we find a local minimum at $x=0.013$ ($m^*=0.084m_e$), which agrees very well with the LCINS-predicted minimum at $x=0.010$ ($m^*=0.1m_e$). We also find a local maximum at $x=0.017$ ($m^*=0.164m_e$) which is in very good agreement with the LCINS-predicted maximum at $x=0.018$ ($m^*=0.18m_e$). Indeed, our observed nonmonotonic increase in m^* with x agrees very well with the x dependence (maxima at $x=0.004$ and $x=0.018$, minimum at $x=0.010$)

predicted by the LCINS model. Our m^* values are also in good agreement with experimental values from Masia *et al.*⁷ for $x=0.014$ but are significantly lower for $x=0.011$. The discrepancy for $x=0.011$ can be resolved with corrections for x from the interstitial model by Reason *et al.*,¹⁵ shifting m^* values by Masia *et al.* to higher x . In the very dilute limit, the decrease in m^* , reported by Young *et al.*,⁴ is likely to be an artifact of the parabolic band-structure assumption for highly doped GaAsN.

IV. CONCLUSION

In summary, we have determined the T dependence of m^* for a set of GaAs_{1-x}N_x alloy films with x values ranging from 0 to 0.018. We observe a nonmonotonic dependence of m^* on

x and an increasing m^* T dependence with x , both of which cannot be explained by a simple two-state BAC model. Instead, the data is in good agreement with the LCINS model, which takes into account several N-related states and their interaction with the GaAs CBE.

ACKNOWLEDGMENTS

We gratefully acknowledge support of the Science Foundation Ireland and the National Science Foundation through Grants DMR-0606406, DMR-0604549, and DMR-1006835, monitored by LaVerne Hess. C.U., R.S.G., and Y.J. were supported in part by the Center for Solar and Thermal Energy Conversion, an Energy Frontier Research Center funded by the U.S. Department of Energy, Office of Science, Office of Basic Energy Sciences under Award No. DE-SC0000957.

*Corresponding author; rsgold@umich.edu

- ¹S. Kurtz, A. Allerman, C. Seager, R. Sieg, and E. Jones, *Appl. Phys. Lett.* **77**, 400 (2000).
- ²R. Mouillet, L.-A. de Vaulchier, E. Deleporte, Y. Guldner, L. Travers, and J.-C. Harmand, *Solid State Commun.* **126**, 333 (2003).
- ³J. Ibáñez, R. Cuscó, E. Alarcón-Lladó, L. Artús, A. Patanè, D. Fowler, L. Eaves, K. Uesugi, and I. Suemune, *J. Appl. Phys.* **103**, 103528 (2008).
- ⁴D. L. Young, J. F. Geisz, and T. J. Coutts, *Appl. Phys. Lett.* **82**, 1236 (2003).
- ⁵M. Reason, Y. Jin, H. A. McKay, N. Mangan, D. Mao, R. S. Goldman, X. Bai, and C. Kurdak, *J. Appl. Phys.* **102**, 103710 (2007).
- ⁶S. Fahy, A. Lindsay, H. Ouerdane, and E. P. O'Reilly, *Phys. Rev. B* **74**, 035203 (2006).
- ⁷F. Masia, G. Pettinari, A. Polimeni, M. Felici, A. Miriametro, M. Capizzi, A. Lindsay, S. B. Healy, E. P. O'Reilly, A. Cristofoli, G. Bais, M. Piccin, S. Rubini, F. Martelli, A. Franciosi, P. J. Klar, K. Volz, and W. Stolz, *Phys. Rev. B* **73**, 073201 (2006).
- ⁸C. Skierbiszewski, I. Gorczyca, S. P. Lepkowski, J. Lusakowski, J. Borysiuk, and J. Toivonen, *Semicond. Sci. Technol.* **19**, 1189 (2004).
- ⁹G. Allison, S. Spasov, A. Patane, L. Eaves, N. V. Kozlova, J. Freudenberger, M. Hopkinson, and G. Hill, *Phys. Rev. B* **77**, 125210 (2008).
- ¹⁰A. Lindsay and E. P. O'Reilly, *Phys. Rev. Lett.* **93**, 196402 (2004).
- ¹¹W. Shan, W. Walukiewicz, J. W. Ager III, E. E. Haller, J. F. Geisz, D. J. Friedman, J. M. Olson, and S. R. Kurtz, *Phys. Rev. Lett.* **82**, 1221 (1999).
- ¹²M. Reason, H. A. McKay, W. Ye, S. Hanson, R. S. Goldman, and V. Rotberg, *Appl. Phys. Lett.* **85**, 1692 (2004).
- ¹³W. Ye, S. Hanson, M. Reason, X. Weng, and R. S. Goldman, *J. Vac. Sci. Technol. B* **23**, 1736 (2005).
- ¹⁴H. Q. Hou, B. W. Liang, T. P. Chin, and C. W. Tu, *Appl. Phys. Lett.* **59**, 292 (1991).
- ¹⁵M. Reason, X. Weng, W. Ye, D. Dettling, S. Hanson, G. Obeidi, and R. S. Goldman, *J. Appl. Phys.* **97**, 103523 (2005).
- ¹⁶C. Herring, *Phys. Rev.* **96**, 1163 (1954).
- ¹⁷G. Homm, P. J. Klar, J. Teubert, and W. Heimbrod, *Appl. Phys. Lett.* **93**, 042107 (2008).
- ¹⁸Y. Jin, R. M. Jock, H. Cheng, Y. He, A. M. Mintarov, Y. Wang, C. Kurdak, J. L. Merz, and R. S. Goldman, *Appl. Phys. Lett.* **95**, 062109 (2009).
- ¹⁹S. G. Spruytte, M. C. Larson, W. Wampler, C. W. Coldren, H. E. Petersen, and J. S. Harris, *J. Cryst. Growth* **227-228**, 506 (2001).
- ²⁰D. L. Rode and S. Knight, *Phys. Rev. B* **3**, 2534 (1971).
- ²¹Y. Jin, Y. He, H. Cheng, R. M. Jock, T. Dannecker, M. Reason, A. M. Mintarov, C. Kurdak, J. L. Merz, and R. S. Goldman, *Appl. Phys. Lett.* **95**, 092109 (2009).
- ²²J. S. Blakemore, *J. Appl. Phys.* **53**, R123 (1982).
- ²³J. Shah, R. C. Leite, and J. F. Scott, *Solid State Commun.* **8**, 1089 (1970).
- ²⁴H. Ehrenreich, *Phys. Rev.* **120**, 1951 (1960).
- ²⁵W. G. Spitzer and H. Y. Fan, *Phys. Rev.* **106**, 882 (1957).
- ²⁶W. G. Spitzer and J. M. Wehlan, *Phys. Rev.* **114**, 59 (1959).
- ²⁷M. Cardona, *Phys. Rev.* **121**, 752 (1961).
- ²⁸J. M. Chamberlain and R. A. Stradling, *Solid State Commun.* **7**, 1275 (1969).
- ²⁹G. Lindemann, R. Lassnig, W. Seidenbusch, and E. Gornik, *Phys. Rev. B* **28**, 4693 (1983).
- ³⁰Q. H. F. Vrehen, *J. Phys. Chem. Solids* **29**, 129 (1968).
- ³¹H. Hazama, T. Sugimasa, T. Imachi, and C. Hamaguchi, *J. Phys. Soc. Jpn.* **55**, 1282 (1986).
- ³²D. Schneider, K. Fricke, J. Schulz, G. Irmer, and M. Wenzel, *Wiss. Ber. HMFA Braunschweig* **14**, 67 (1996).
- ³³R. A. Stradling and R. A. Wood, *J. Phys. C* **3**, L94 (1970).
- ³⁴J. Heremans, V. Jovovic, E. Toberer, A. Saramat, K. Kurosaki, A. C. S. Yamanaka, and G. Snyder, *Science* **321**, 554 (2008).